

Adaptive Sliding Mode Control for Vehicle Platoons with State-Dependent Friction Uncertainty

Thesis submitted in partial fulfillment
of the requirements for the degree of

Master of Science in
Computer Science and Engineering
by Research

by

RISHABH DEV YADAV

2021701030

RISHABH.YADAV@RESEARCH.IIIT.AC.IN



International Institute of Information Technology
Hyderabad - 500 032, INDIA

June 2023

This manuscript is based on the author's MSc thesis (IIIT Hyderabad, 2023).

A shorter version of this work appeared in the IEEE International Conference on Advanced Robotics (ICAR 2021).

Title: Adaptive Sliding Mode Control for Autonomous Vehicle Platoon under Unknown Friction Forces.

Authors: Rishabh Dev Yadav, Viswa N. Sankaranarayanan, Spandan Roy

DOI: [10.1109/ICAR53236.2021.9659441](https://doi.org/10.1109/ICAR53236.2021.9659441)

Copyright © RISHABH DEV YADAV, 2023

All Rights Reserved

International Institute of Information Technology
Hyderabad, India

CERTIFICATE

It is certified that the work contained in this thesis, titled “Adaptive Sliding Mode Control for Autonomous Vehicle Platoon under Unknown Friction Forces” by RISHABH DEV YADAV, has been carried out under my supervision and is not submitted elsewhere for a degree.

Date

Adviser: Prof. SPANDAN ROY

To My Family and Teachers

Acknowledgments

Firstly, I express my gratitude to Prof. Kamalakar Karlapalem, AARG LAB, IIIT Hyderabad, who gave me the opportunity to explore and learn robotics at IIIT Hyderabad. I also appreciate the technical and philosophical discussions I had with Professor K Madhava Krishna. I am especially grateful to my advisor, Dr Spandan Roy, who introduced me to Robotics and Control and provided me with guidance. Without him, I would not have gained a fundamental perspective on how to contribute to research.

I am especially thankful to my family for their unwavering support in all my endeavors, allowing me the freedom to explore my interests and grow. Their love and encouragement are incomparable.

During my time at RRC, many of my colleagues have helped me to grasp and understand the concepts in my field. I would like to thank Viswa N. Sankaranarayanan, B.V.S.G. Suraj, Swati Dantu, Sudarshan, and all my colleagues at RRC who have supported and believed in me. I am grateful to the Robotics Research Center (RRC) for welcoming me with open arms. I am fortunate to have had great friends who have pushed me beyond my comfort zone and encouraged me to take research seriously. I thank everyone in RRC and AARG lab for their acceptance, inspiration, and motivation from the very beginning.

Lastly, I would like to thank the institute for providing a platform for aspiring researchers to pursue their dreams and develop themselves in the process. I also appreciate the thesis examiners for their valuable feedback, which helped me improve this thesis.

Thank you all.

Abstract

Multi-robot formation control has various applications in domains such as vehicle troops, platoons, payload transportation, and surveillance. Maintaining formation in a vehicle platoon requires designing a suitable control scheme that can tackle external disturbances and uncertain system parameters while maintaining a predefined safe distance between the robots. A crucial challenge in this context is dealing with the unknown/uncertain friction forces between wheels and the ground, which vary with changes in road surface, wear in tires, and speed of the vehicle. Although state-of-the-art adaptive controllers can handle a priori bounded uncertainties, they struggle with accurately modeling and identifying frictional forces, which are often state-dependent and cannot be a priori bounded.

This thesis proposes a new adaptive sliding mode controller for wheeled mobile robot-based vehicle platoons that can handle the unknown and complex behavior of frictional forces without prior knowledge of their parameters and structures. The controller uses the adaptive sliding mode control techniques to regulate the platoon's speed and maintain a predefined inter-robot distance, even in the presence of external disturbances and uncertain system parameters. This approach involves a two-stage process: first, the kinematic controller calculates the desired velocities based on the desired trajectory; and second, the dynamics model generates the commands to achieve the desired motion. By separating the kinematics and dynamics of the robot, this approach can simplify the control problem and allow for more efficient and robust control of the wheeled mobile robot.

The stability of the closed-loop system employing both the proposed controllers are studied analytically via Lyapunov theory. The effectiveness of the proposed controller is demonstrated through simulations using Gazebo, a popular robot simulation tool. The simulations show that the proposed controller outperforms existing state-of-the-art controllers in terms of stability, convergence, and robustness to changes in frictional forces. The simulations also demonstrate the controller's ability to maintain formation under various road conditions, including slopes, curves, and rough terrain.

Contents

Chapter	Page
1 Introduction	1
1.1 Autonomous Vehicle Platoon	2
1.2 System Representation	3
1.2.1 Reference Frames	3
1.2.2 Kinematic Model	4
1.2.3 Dynamic model	5
1.2.4 Friction Model	7
1.3 Control of multiple mobile robots	8
1.3.1 Motivation	8
1.3.2 Related Works	8
1.3.3 Contribution	9
1.4 Organization of the Thesis	9
2 Adaptive Sliding Mode Control for Autonomous Vehicle Platoon under Unknown Friction Forces	11
2.1 Introduction	11
2.2 CONTROL FORMULATION	12
2.2.1 Kinematic Control Design	12
2.2.2 PROPOSED DYNAMIC CONTROLLER DESIGN	13
2.2.3 Force Control	13
2.2.4 Torque Control	15
2.3 Stability Analysis of The Proposed Controller	16
3 SIMULATION RESULTS	19
3.0.1 Simulation Scenario	19
3.0.2 Parameter Selection	21
3.0.3 Results and Analysis	21
4 Conclusion and Future Work	27
Bibliography	31

List of Figures

Figure	Page
1.1 Platoonig. Source: Wikipedia	2
1.2 Schematic of a two-wheeled nonholonomic mobile robot	4
1.3 Coulomb + Viscous friction model	7
3.1 Multi-Robot Platoon Representation	19
3.2 Custom Arena	20
3.3 Position tracking error comparison for Robot 1.	22
3.4 Position tracking error comparison for Robot 2.	22
3.5 Position tracking error comparison for Robot 3.	23
3.6 Trajectory tracking comparison for Robot 1.	24
3.7 Trajectory tracking comparison for Robot 2.	24
3.8 Trajectory tracking comparison for Robot 3.	25
3.9 (a) Gap error comparison between Robot 1 and Robot 2. (b) Gap error comparison between Robot 2 and Robot 3.	25

List of Tables

Table	Page
3.1 Performance Comparison for Trajectory Tracking	26
3.2 Performance Comparison for Gap Maintenance	26

Chapter 1

Introduction

The field of robotics has captured people's imaginations due to its potential for machines to replace humans in everyday tasks. One of the main benefits of robotics is the inefficiency of humans in performing repetitive tasks. Machines can perform these tasks without constraints such as boredom or distraction. Additionally, robots can transcend the mechanical limitations of humans, making them ideal for tasks that are physically demanding or hazardous.

The development of robots has followed a similar path to the evolution of living beings. Initially, robots were designed for specific operations, and humanoid fantasies were seen as impractical with the technology available at the time. Robots came in various mechanical forms with task-specific features similar to living creatures. One significant step in the evolution of robotics was the development of autonomous systems that could perform tasks without human control. This development led to the need for a new science stream called control, which is essential for the functioning of autonomous systems.

One of the most significant applications of autonomous systems is in the field of autonomous vehicles. These vehicles have been brought to life through advances in control techniques and are used for research and commercial purposes. Autonomous vehicles come in various forms, including cars, ships, and quadrotors. While the use cases for aerial and marine robots are limited due to safety constraints, road vehicles equipped with autopilot features are already in use, and major automobile manufacturers are shifting their focus towards autonomous vehicles.

The control of autonomous vehicles encompasses a broad range of activities, from high-level control that selects an optimal trajectory to low-level control that determines appropriate actuator inputs. Robotics and control engineering are two closely related fields that have played an instrumental role in shaping our modern world. Robotics involves the design, construction, operation, and use of robots to perform a wide range

of tasks, from manufacturing and assembly to exploration and space travel. Control engineering, on the other hand, focuses on designing and implementing control systems to manage and regulate complex processes, ensuring that they are efficient, safe, and reliable.

The integration of robotics and control engineering has led to many significant advancements in various industries. For example, in manufacturing, robots and automation have transformed production lines, allowing for faster and more efficient assembly of products. Robots can perform tasks that are repetitive, dangerous, or require high precision, which reduces the risk of injury and improves quality control. Control engineering is used to optimize and manage these complex systems, ensuring that they operate efficiently and safely.

Parts of this work were previously presented in [1]; the present manuscript provides a consolidated and expanded exposition with complete derivations and simulations

1.1 Autonomous Vehicle Platoon

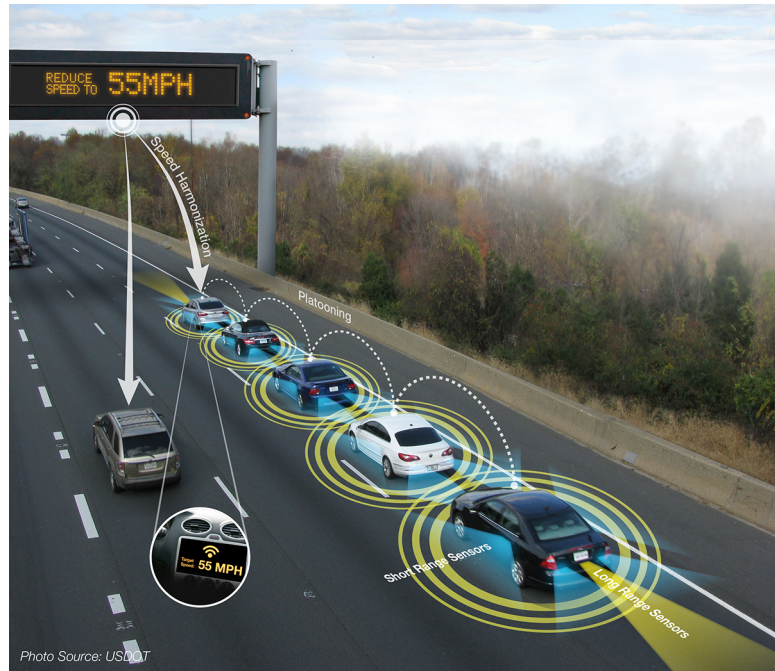


Figure 1.1: Platoonig. Source: Wikipedia

Multi-wheeled mobile robot platoons are a type of robotic system that has the potential to revolutionize the way goods are transported in logistics and distribution networks.

These platoons consist of a group of autonomous vehicles that can operate together in a coordinated manner, following a lead vehicle or a predetermined path. This technology is being developed by various research institutions and companies around the world, with the aim of reducing transportation costs and increasing efficiency.

The benefits of using multi-wheeled mobile robot platoons are numerous. First and foremost, they can increase transportation efficiency and reduce costs. By coordinating the movements of several vehicles, platoons can travel at a constant speed and maintain a safe following distance, reducing the need for drivers and optimizing fuel consumption. This can lead to significant savings for logistics and distribution companies.

Another benefit of multi-wheeled mobile robot platoons is their potential to reduce traffic congestion and improve safety on roads. By coordinating their movements, these platoons can reduce the number of vehicles on the road, decreasing the likelihood of accidents and reducing travel times for other drivers.

Additionally, these platoons can operate autonomously, eliminating the need for human drivers. This can lead to increased safety, as there is less risk of accidents caused by human error. It can also lead to cost savings for logistics and distribution companies, as they will not need to pay for drivers' salaries, benefits, and training.

1.2 System Representation

The main components involved in modeling a robotic system, namely, representing the model, defining reference frames with state variables, and developing kinematic and dynamic dynamic equations. Although there are various approaches to modeling dynamics in each of these sections, the focus will be on the method employed in this work.

1.2.1 Reference Frames

In order to describe the position of the robot Inertial Coordinate System (X_I, Y_I) and Robot Coordinate System (X_r, Y_r) frames are shown in Figure (1.2). The Inertial Coordinate System is a global frame which remains fixed in the environment or plane where the wheeled mobile robot (WMR) operates. It serves as the benchmark for reference. While, the Robot Coordinate System is local frame which is affixed to the mobile robot and moves along with it.

The position of any point on the robot can be defined in the robot frame and the inertial frame as $X^r = [x^r, y^r, \theta^r]^T$ and $X^I = [x^I, y^I, \theta^I]^T$ respectively. The important

issue that needs to be explained at this stage is the relation between these two frames. Then, the two coordinates are related by the following transformation

$$X^I = R(\theta)X^r \quad (1.1)$$

$$\text{where } R(\theta) = \begin{bmatrix} \cos(\theta) & -\sin(\theta) & 0 \\ \sin(\theta) & \cos(\theta) & 0 \\ 0 & 0 & 1 \end{bmatrix}$$

The robot position and orientation in the Inertial Frame can be defined as $q^I = [x_a, y_a, \theta]^T$

1.2.2 Kinematic Model

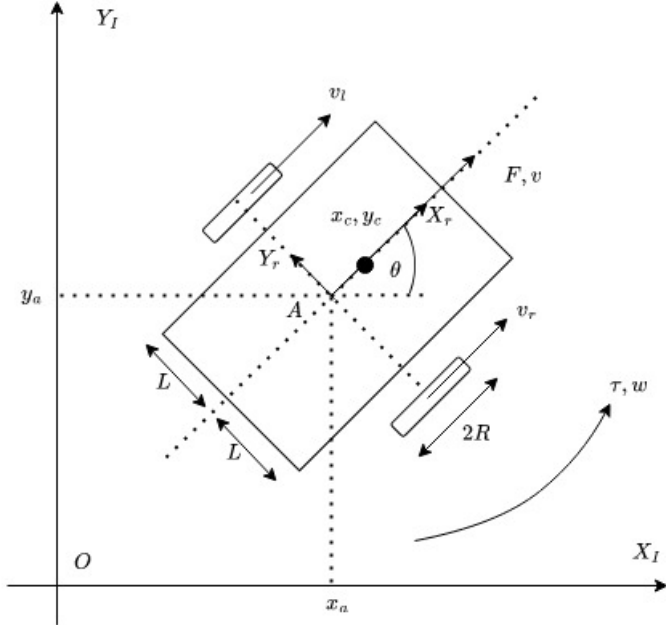


Figure 1.2: Schematic of a two-wheeled nonholonomic mobile robot

Kinematic modeling involves analyzing the movement of mechanical systems while disregarding the forces that influence the movement. In the case of the mobile robot, the primary goal of kinematic modeling is to express the robot's velocities in relation to the velocities of its driving wheels and the robot's geometric characteristics.

Let v_r and v_l denote the right and left wheel linear speed respectively.

$$v_r = R\dot{\phi}_r \quad (1.2a)$$

$$v_l = R\dot{\phi}_l \quad (1.2b)$$

where $\dot{\phi}_r$ and $\dot{\phi}_l$ are angular speed of right and left wheel respectively; R is wheel radius. The linear velocity v of the robot in the Robot Frame is the average of the linear velocities of the two wheels,

$$v = \frac{v_r + v_l}{2} = R\frac{\dot{\phi}_r + \dot{\phi}_l}{2} \quad (1.3)$$

and the angular velocity of the robot is

$$w = \frac{v_r - v_l}{2L} = R\frac{\dot{\phi}_r - \dot{\phi}_l}{2} \quad (1.4)$$

where $2L$ denote the width of the robot (cf. Fig. 1.2). The velocities in the robot frame can now be represented in terms of the center-point A velocities in the robot frame as follows:

$$\dot{x}_a^r = v; \quad \dot{y}_a^r = 0; \quad \dot{\theta} = w \quad (1.5)$$

The robot velocities in the inertial frame can be written as

$$\dot{q}^I = \begin{bmatrix} \dot{x}_a \\ \dot{y}_a \\ \dot{\theta} \end{bmatrix} = R(\theta) \begin{bmatrix} \frac{R}{2} & \frac{R}{2} \\ 0 & 0 \\ \frac{R}{2b} & -\frac{R}{2b} \end{bmatrix} \begin{bmatrix} \dot{\phi}_r \\ \dot{\phi}_l \end{bmatrix} \quad (1.6)$$

For each robot in the platoon (cf. Fig. 1.2), $q = [x, y, \theta]^T$ represents the generalized state with (x, y) is the robot position in the global inertial frame, and θ being its heading angle (yaw); $u = [v, \omega]^T$ is the control input where v is the linear velocity and ω is the angular velocity of the robot. The typical kinematic model of such system is given by

$$\dot{q} = \begin{bmatrix} \cos(\theta) & 0 \\ \sin(\theta) & 0 \\ 0 & 1 \end{bmatrix} u. \quad (1.7)$$

1.2.3 Dynamic model

The field of dynamics involves examining how mechanical systems move while accounting for the various forces that impact their motion. This differs from kinematics, which does not take these forces into account. In order to analyze the motion of the mobile

robot and develop motion control algorithms, it is crucial to have a dynamic model of the system.

Deriving system equations of motion via Lagrangian method rely on the following equation:

$$\frac{d}{dt}\left(\frac{\partial L}{\partial \dot{q}_i}\right) - \frac{\partial L}{\partial q_i} = F - \Gamma^T(q)\gamma \quad (1.8)$$

where $L = T - P$ is the Lagrangian function; T and P represents kinetic energy and potential energy of system respectively; q_i are generalized coordinate; F is the generalized force vector. However, since the robot is moving in the (X_I, Y_I) plane, the potential energy of the robot is considered to be zero i.e. $P = 0$.

A non-holonomic differential drive robot with n generalized coordinates (q_1, q_2, \dots, q_n) and subject to constraints can be described by the following equations of motion:

$$M(q)\ddot{q} + V(q, \dot{q})\dot{q} + F(\dot{q}) + G(q) + \tau_d = B(q)\tau_u - \Gamma^T(q)\gamma \quad (1.9)$$

where $M(q)$ an $n \times n$ symmetric positive definite inertia matrix, $V(q, \dot{q})$ is the centripetal and coriolis matrix, $F(\dot{q})$ is the surface friction matrix, $G(q)$ is the gravitational vector, τ_d is the vector of bounded unknown disturbances including unstructured unmodeled dynamics, $B(q)$ is the input matrix, τ_u is the input vector, Γ is the constraints matrix, γ is the vector of Lagrange multipliers associated with the constraints.

Ignoring the distance between centre of mass of the robot and origin of the local coordinate frame attached to the mobile robot, the standard dynamic model of the system is given by

$$m\dot{v} + f_v + d_v = F, \quad \text{with } f_v = f_r + f_l, \quad (1.10a)$$

$$J\dot{\omega} + f_w + d_w = \tau, \quad \text{with } f_w = f_r + f_l. \quad (1.10b)$$

Here m and J denote the mass and the moment of inertia of the robot; d_v and d_w represent bounded external disturbances; f_v and f_w are the frictional force and frictional torque respectively generated at the right (f_r) and left (f_l) wheel; (F, τ) denote the control input.

Let τ_r and τ_l be the right and left wheel torque respectively and R be the radius of the wheel. Then, the following holds

$$\begin{bmatrix} F \\ \tau \end{bmatrix} = \frac{1}{R} \begin{bmatrix} (\tau_r + \tau_l) \\ (\tau_r - \tau_l)L \end{bmatrix}. \quad (1.11)$$

1.2.4 Friction Model

Friction is the force that opposes motion between two surfaces in contact. Two common types of friction models are Coulomb friction and viscous friction. While both models describe the behavior of friction, they differ in their underlying assumptions and mathematical expressions.

Coulomb friction, also known as dry friction or static friction, is a simple model that assumes that the friction force between two surfaces in contact is proportional to the normal force pressing the surfaces together. The model further assumes that the friction force is independent of the sliding speed and that it only acts when the surfaces are in contact and stationary relative to each other. Once the surfaces start moving relative to each other, the friction force decreases and becomes proportional to the kinetic friction coefficient, which is typically lower than the static friction coefficient.

Viscous friction, also known as dynamic or fluid friction, is a more complex model that assumes that the friction force is proportional to the velocity of the surfaces relative to each other. This model is often used to describe the behavior of fluids, such as air or liquids, but can also be applied to solid materials. The viscous friction coefficient depends on the viscosity of the fluid or the deformation properties of the solid material and can vary with temperature and other factors.

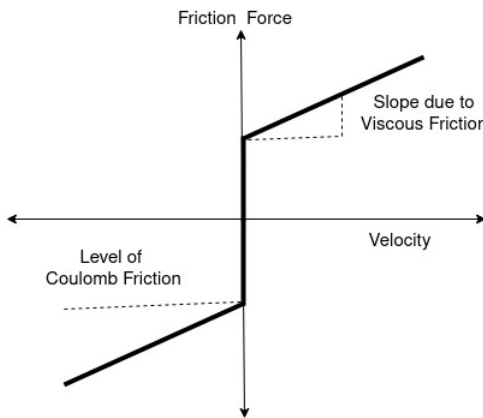


Figure 1.3: Coulomb + Viscous friction model

The mathematical expressions for Coulomb and viscous friction are also different. Coulomb friction is typically expressed as a constant static friction coefficient and a lower kinetic friction coefficient, while viscous friction is expressed as a linear function of the velocity between the surfaces.

While both models have their limitations, they are useful for understanding and predicting the behavior of friction in different scenarios. The general friction model for a moving body considering the static Coulomb friction (f_k) and the viscous friction (f_c) can be represented as $f_r = f_k + f_c$ (cf. 1.3). The friction forces f_v and f_w in (1.10a) and (1.10b) can be rewritten as

$$f_v = (f_{kr} + f_{cr}v_r) + (f_{kl} + f_{cl}v_l), \quad (1.12a)$$

$$f_w = ((f_{kr} + f_{cr}v_r) - (f_{kl} + f_{cl}v_l))L \quad (1.12b)$$

where f_{ki} and f_{ci} are coulomb and viscous friction respectively for wheel having speed v_i with $i = r, l$ as in (1.3) and (1.4).

1.3 Control of multiple mobile robots

1.3.1 Motivation

Cooperative mobile multi-robot systems have gained significant attention due to their advantages over single-robot systems, such as better efficiency, high tolerance, redundancy, and manoeuvrability [2, 3]. These multi-robot systems have a broad range of applications, including search and rescue, exploration, navigation, security and surveillance, precision agriculture, and payload transportation [4–7]. One specific application is the platoon of autonomous vehicles, where multiple agents/robots/vehicles follow a common path in a shared environment. The control objective of such formation control is often decentralized [8], where the aim is to maintain a desired line-of-sight range between each vehicle and its predecessor while proceeding along a given trajectory [9]. However, controlling these systems under parametric uncertainties and unmodelled dynamics is still a significant challenge and an open problem.

1.3.2 Related Works

When it comes to autonomous platooning, the accuracy of formation control is heavily influenced by vehicle dynamics and external disturbances, particularly at higher speeds. The use of a simple Coulomb friction model is inadequate to capture the complex relationship between tyre wear and friction forces, as evidenced by previous studies [10–12]. However, accurately parameterizing this phenomenon in real-world situations is challenging, if not impossible, due to the variability of friction forces caused by factors such as changes in payload quantity, road conditions, and tyre distortion.

Advanced control strategies such as interpolating control [13], distributed formation control [14], intervehicle distance control [15], and robust control [16] have been developed to handle the dynamics of vehicles for both longitudinal and lateral control in automatic platoon formation. However, these strategies require prior knowledge of system parameters. To address this limitation, two-stage tracking controllers have been used for wheeled mobile robots [17–19], combining a kinematic controller with an adaptive sliding mode controller (ASMC). However, these controllers can only handle bounded uncertainties, and frictional forces, which are state-dependent, do not satisfy this requirement [20, 21].

Therefore, there is a need for an adaptive control solution that can handle state-dependent unknown dynamics without prior knowledge for a multi-robot platoon system. Current research in this area has been focused on using a combination of a kinematic controller and ASMC for tracking control. However, these methods have been limited in their ability to handle unbounded uncertainties, which can arise due to the state-dependent nature of frictional forces. To overcome this limitation, new research is needed to develop adaptive control methods that can handle state-dependent uncertainties in multi-robot platoon systems. This research should focus on developing controllers that can adapt to changing conditions in real-time, without requiring prior knowledge of system parameters. In addition, these controllers should be designed to be robust to unbounded uncertainties, such as those arising from frictional forces.

1.3.3 Contribution

Based on the limitations of current control methods for multi-robot platoon systems, a new framework ASMC is proposed. This framework does not require prior knowledge of system dynamics, including inertia parameters, frictional forces, and external disturbances. The stability of the closed-loop system is analyzed using the Lyapunov method, and simulation results show that the proposed method outperforms current state-of-the-art control methods for multi-robot platoon formation control.

1.4 Organization of the Thesis

The thesis is organized into four chapters. A brief summary of each chapter is mentioned below.

- Chapter 1: This introductory chapter gives an overview of wheeled robotics, kinematic and dynamic modelling and state-of-the-art control strategies. It briefly

describes the motivation for this research, the problem orientation, the pertaining gaps in the literature, the main contributions and an outline of the thesis.

- Chapter 2: The chapter explains a new adaptive sliding mode controller for WMR-based vehicle platoons that can handle unknown and complex frictional forces. The controller maintains a predefined inter-robot distance and regulates the platoon's speed despite external disturbances and uncertain system parameters. The approach involves a two-stage process of kinematic and dynamic controllers to achieve the desired motion. This allows for more efficient and robust control of the mobile robot. The stability of the closed-loop system using the proposed controllers is studied using Lyapunov theory.
- Chapter 3: In this chapter the proposed controller's effectiveness was demonstrated using Gazebo simulations results, showing it outperformed state-of-the-art controllers in terms of stability, convergence, and robustness to frictional force changes. The performance is compared via error plots and root mean-squared (RMS) error.
- Chapter 4: This chapter concludes the thesis by summarizing the various contributions brought out by this thesis.

Chapter 2

Adaptive Sliding Mode Control for Autonomous Vehicle Platoon under Unknown Friction Forces

2.1 Introduction

In cases where the system parameters are unknown, state-of-art control laws have been employed to handle a priori bounded uncertainties. Unfortunately, frictional forces generally do not adhere to such uncertainty settings due to their state-dependent nature. Prior studies have been unable to handle state-dependent unknown dynamics without prior knowledge, leaving a gap in the field. Therefore, a solution for multi-robot platoon systems that can handle state-dependent unknown dynamics without prior knowledge is still lacking.

Toward this direction, the proposed adaptive control solution has the following major contributions:

- The study introduces an ASMC framework to address state-dependent dynamic factors such as frictional and inertial forces, as well as external disturbances, in each vehicle of a platoon.
- The closed-loop stability of the system is analysed via Lyapunov-based method and comparative simulation results suggest significant improvement in tracking accuracy of the proposed scheme compared to the state of the art.

The rest of the chapter is organised as follows: Section 2.2 describes the controller design; Section 2.3 details the proposed control stability analysis.

2.2 CONTROL FORMULATION

The platoon control problem involves multiple vehicles, each with their own trajectory to follow. Except for the leading vehicle, each follower calculates its next waypoint based on the position of the vehicle in front of it. The focus of this work is on controlling each vehicle, which is considered a nonholonomic WMR, to follow the desired path rather than planning the path for each robot.

Controlling a nonholonomic WMR effectively requires considering both kinematic and dynamic model-based controllers [17–19]. In this approach, the linear and angular velocity derived from the kinematic controller are used as the desired trajectory in the dynamic model. However, since parametric uncertainty can only be captured in the dynamic model, the novelty of this work lies in designing an ASMC for the dynamic model while using the standard kinematic controller as in previous works [22–24].

2.2.1 Kinematic Control Design

The kinematic control design objective is to follow a time-varying reference trajectory $q_r(t) = [x_r(t), y_r(t), \theta_r(t)]^T$.

The following standard assumption is made:

Assumption 1 The desired trajectories $x_r(t)$ and $y_r(t)$ are designed to be sufficiently smooth and bounded.

The posture tracking error of the mobile robot $q_e(t)$ is defined as

$$q_e(t) = [e_1(t), e_2(t), e_3(t)]^T \quad (2.1)$$

where

$$\begin{bmatrix} e_1(t) \\ e_2(t) \\ e_3(t) \end{bmatrix} = \begin{bmatrix} \cos \theta(t) & \sin \theta(t) & 0 \\ -\sin \theta(t) & \cos \theta(t) & 0 \\ 0 & 0 & 1 \end{bmatrix} \begin{bmatrix} x_r(t) - x(t) \\ y_r(t) - y(t) \\ \theta_r(t) - \theta(t) \end{bmatrix}. \quad (2.2)$$

In order to be more concise, we will eliminate the time-related aspects of the functions whenever feasible. Using (1.7), the time derivative of (2.2) leads to

$$\begin{bmatrix} \dot{e}_1 \\ \dot{e}_2 \\ \dot{e}_3 \end{bmatrix} = v \begin{bmatrix} -1 \\ 0 \\ 0 \end{bmatrix} + \omega \begin{bmatrix} e_2 \\ -e_1 \\ -1 \end{bmatrix} + \begin{bmatrix} v_d \cos(e_3) \\ v_d \sin(e_3) \\ \omega_d \end{bmatrix}, \quad (2.3)$$

where $u_d = [v_d, \omega_d]^T$ denotes the reference (desired) time-varying linear and angular velocity.

Following [22–24], we used the following backstepping method based kinematic tracking control law

$$\begin{bmatrix} v_c \\ \omega_c \end{bmatrix} = \begin{bmatrix} v_d \cos(e_3) + k_1 e_1 \\ \omega_d + k_2 v_d e_2 + k_3 v_d \sin(e_3) \end{bmatrix} \quad (2.4)$$

where k_1, k_2 and k_3 are positive design constants.

As mentioned earlier, the main contribution of the work lies in designing the dynamic controller and the corresponding control problem is discussed subsequently.

2.2.2 PROPOSED DYNAMIC CONTROLLER DESIGN

Remark 1 (State-dependent forces) It is crucial to note that viscous friction being proportional to the velocity v of the vehicle, the friction forces are state-dependent and thus, cannot be bounded a priori [25–28]. Such consideration segregates this work from the state-of-the-art adaptive solutions [17–19] relying on a priori bounded dynamical forces.

With this observation, we present the following assumption on system dynamics uncertainty, which acts as a control design challenge.

Assumption 2 (Uncertainty setting) The system dynamics terms m, J, d_v, d_w and their bounds are unknown for control design.

Following the system dynamics structure (1.10), the proposed control framework is divided into two parts, namely, force control and torque control as detailed in the following two subsections. It is noteworthy that the co-design approach of force and torque control are not independent; rather they are interconnected via the uncertainty structures (cf. (2.10) and (2.17)) and thereby to be designed simultaneously.

Let us define the linear velocity tracking error e_v and the angular velocity tracking error e_ω as

$$e_v \triangleq v - v_c, \quad e_\omega \triangleq \omega - \omega_c. \quad (2.5)$$

2.2.3 Force Control

Let the sliding variable be designed as

$$s_v(t) = e_v(t) + \phi_v \int_0^t e_v(\psi) d\psi, \quad (2.6)$$

where ϕ_v is a positive design scalar. Multiplying the time derivative of (2.6) by m and using (1.10) gives

$$m\dot{s}_v = m(\dot{v} - \dot{v}_c + \phi_v e_v) = F + \epsilon_v, \quad (2.7)$$

where $\epsilon_v \triangleq -(d_v + m\dot{v}_c + f_v - m\phi_v e_v)$ represents the overall uncertainty in force dynamics with its upper bound structure computed as

$$|\epsilon_v| \leq \overline{d_v} + m(|\dot{v}_c| + |\phi_v||e_v|) + |f_v|, \quad (2.8)$$

where $|d_v| \leq \overline{d_v}$. Substituting the relations $v_r = \frac{2v+\omega L}{2}$ and $v_l = \frac{2v-\omega L}{2}$ from (1.3) and (1.4) into (1.12), the upper bound structure (2.8) can be simplified to

$$\begin{aligned} |\epsilon_v| \leq & \overline{d_v} + m(|\dot{v}_c| + |\phi_v||e_v|) + |f_{kr}| + |f_{kl}| + \\ & |v|(|f_{cr}| + |f_{cl}|) + (L/2)|\omega|(|f_{cr}| + |f_{cl}|). \end{aligned} \quad (2.9)$$

Further, let us define $\xi_v \triangleq [e_v, \int_0^t e_v(\psi) d\psi]^T$ and $\xi_\omega \triangleq [e_\omega, \int_0^t e_\omega(\psi) d\psi]^T$. Then, using the inequalities $|\xi_v| \geq |e_v|$ and $|\xi_\omega| \geq |e_\omega|$ and substituting $v = e_v + v_c$ and $\omega = e_\omega + \omega_c$ from (2.5) into (2.9) one obtains

$$|\epsilon_v| \leq K_{v0}^* + K_{v1}^*|\xi_v| + K_{\omega2}^*|\xi_\omega| \quad (2.10)$$

$$\begin{aligned} \text{where } K_{v0}^* \triangleq & \overline{d_v} + m|\dot{v}_c| + |f_{kr}| + |f_{kl}| + |v_c|(|f_{cr}| + |f_{cl}|) \\ & + (L/2)|\omega_c|(|f_{cr}| + |f_{cl}|), \end{aligned}$$

$$K_{v1}^* \triangleq m|\phi_v| + (|f_{cr}| + |f_{cl}|), \quad K_{\omega2}^* \triangleq (L/2)(|f_{cr}| + |f_{cl}|)$$

are unknown scalars.

The force control law is designed as

$$F(t) = -\Lambda_v s_v(t) - \rho_v(t) \operatorname{sgn}(s_v(t)), \quad (2.11a)$$

$$\rho_v(t) = \hat{K}_{v0}(t) + \hat{K}_{v1}|\xi_v| + \hat{K}_{\omega2}|\xi_\omega|, \quad (2.11b)$$

where Λ_v is a positive scalar gain and $(\hat{K}_{v0}(t), \hat{K}_{v1}(t), \hat{K}_{\omega2}(t))$ are estimates of $(K_{v0}^*, K_{v1}^*, K_{\omega2}^*)$ obtained via the following adaptive laws

$$\dot{\hat{K}}_{v0}(t) = |s_v(t)| - \alpha_{v0}\hat{K}_{v0}(t), \quad \hat{K}_{v0}(0) > 0, \quad (2.12a)$$

$$\dot{\hat{K}}_{v1}(t) = |s_v(t)||\xi_v(t)| - \alpha_{v1}\hat{K}_{v1}(t), \quad \hat{K}_{v1}(0) > 0, \quad (2.12b)$$

$$\dot{\hat{K}}_{\omega2}(t) = |s_\omega(t)||\xi_\omega(t)| - \alpha_{\omega2}\hat{K}_{\omega2}(t), \quad \hat{K}_{\omega2}(0) > 0, \quad (2.12c)$$

where $\alpha_{v0}, \alpha_{v1}, \alpha_{\omega2}$ are user-defined positive scalars.

2.2.4 Torque Control

For torque control, the sliding variable is designed as

$$s_\omega(t) = e_\omega(t) + \phi_\omega \int_0^t e_\omega(\psi) d\psi, \quad (2.13)$$

where ϕ_ω is a positive user-defined gain. Multiplying the time derivative of (2.13) by J and using (1.10) yields

$$J\dot{s}_\omega = J(\dot{\omega} - \dot{\omega}_c + \phi\omega_v) = \tau + \epsilon_\omega, \quad (2.14)$$

where $\epsilon_\omega \triangleq -(d_\omega + J\dot{\omega}_c + f_\omega - J\phi_\omega e_\omega)$ is the overall uncertainty for the torque dynamics and it satisfies the following upper bound structure

$$|\epsilon_\omega| \leq \overline{d_\omega} + J(|\dot{\omega}_c| + |\phi_\omega||e_\omega|) + |f_\omega| \quad (2.15)$$

where $|d_\omega| \leq \overline{d_\omega}$. Substituting v_r and v_l from (1.3) and (1.4) into (1.12), then (2.15) is simplified to

$$\begin{aligned} |\epsilon_\omega| \leq & \overline{d_\omega} + J(|\dot{\omega}_c| + |\phi_\omega||e_\omega|) + L(|f_{kr}| + |f_{kl}|) + \\ & |v|L(|f_{cr}| + |f_{cl}|) + |\omega|(L^2/2)(|f_{cr}| + |f_{cl}|). \end{aligned} \quad (2.16)$$

Substituting $v = e_v + v_c$ and $\omega = e_\omega + \omega_c$ in (2.16) and using the inequalities $|\xi_v| \geq |e_v|$ and $|\xi_\omega| \geq |e_\omega|$ the following is obtained from (2.16)

$$|\epsilon_\omega| \leq K_{\omega 0}^* + K_{\omega 1}^*|\xi_\omega| + K_{v2}^*|\xi_v| \quad (2.17)$$

$$\begin{aligned} \text{where } K_{\omega 0}^* \triangleq & \overline{d_\omega} + J|\dot{\omega}_c| + L(|f_{kr}| + |f_{kl}|) + |v_c|L(|f_{cr}| + |f_{cl}|) \\ & + |\omega_c|(L^2/2)(|f_{cr}| + |f_{cl}|), \\ K_{\omega 1}^* \triangleq & J|\phi_\omega| + (L^2/2)(|f_{cr}| + |f_{cl}|), \quad K_{v2}^* \triangleq L(|f_{cr}| + |f_{cl}|) \end{aligned}$$

are unknown scalars.

The torque control law is designed as

$$\tau(t) = -\Lambda_\omega s_\omega(t) - \rho_\omega(t) \operatorname{sgn}(s_\omega(t)), \quad (2.18a)$$

$$\rho_\omega(t) = \hat{K}_{\omega 0}(t) + \hat{K}_{\omega 1}|\xi_\omega| + \hat{K}_{v2}|\xi_v|, \quad (2.18b)$$

where Λ_ω is a user-defined positive scalar gain. The adaptive gains $\hat{K}_{\omega 0}(t)$, $\hat{K}_{\omega 1}(t)$, $\hat{K}_{v2}(t)$ are the estimates of $K_{\omega 0}^*$, $K_{\omega 1}^*$, K_{v2}^* updated as

$$\dot{\hat{K}}_{\omega 0}(t) = |s_\omega(t)| - \alpha_{\omega 0}\hat{K}_{\omega 0}(t), \quad \hat{K}_{\omega 0}(0) > 0, \quad (2.19a)$$

$$\dot{\hat{K}}_{\omega 1}(t) = |s_\omega(t)||\xi_\omega(t)| - \alpha_{\omega 1}\hat{K}_{\omega 1}(t), \quad \hat{K}_{\omega 1}(0) > 0, \quad (2.19b)$$

$$\dot{\hat{K}}_{v2}(t) = |s_v(t)||\xi_v(t)| - \alpha_{v2}\hat{K}_{v2}(t), \quad \hat{K}_{v2}(0) > 0 \quad (2.19c)$$

where $\alpha_{\omega 0}$, $\alpha_{\omega 1}$, α_{v2} are user-defined positive scalars.

Remark 2 The upper bound structures of ϵ_v and ϵ_w in (2.10) and (2.17), respectively, reveal that state-dependencies occur inherently in the system uncertainties via ξ_v and ξ_w . Therefore, the gains ρ_v and ρ_w in (2.11) and (2.18), respectively, are designed according to these state-dependent structures.

2.3 Stability Analysis of The Proposed Controller

Theorem 1 Under the Assumptions 1 and 2, the closed-loop trajectories of (2.7) and (2.14) with control laws (2.11) and (2.18), along with the adaptive laws (2.12) and (2.19) are Uniformly Ultimately Bounded (UUB).

Proof. The closed-loop stability analysis is carried out using the following Lyapunov function

$$V = V_v + V_w, \quad (2.20)$$

$$\text{where } V_v = (1/2) [ms_v^2 + (\hat{K}_{v0} - K_{v0}^*)^2 + (\hat{K}_{v1} - K_{v1}^*)^2 + (\hat{K}_{\omega2} - K_{\omega2}^*)^2],$$

$$V_w = (1/2) [Js_w^2 + (\hat{K}_{w0} - K_{w0}^*)^2 + (\hat{K}_{w1} - K_{w1}^*)^2 + (\hat{K}_{v2} - K_{v2}^*)^2].$$

Using (2.7), the time derivative of V_v yields

$$\begin{aligned} \dot{V}_v &= ms_v \dot{s}_v + (\hat{K}_{v0} - K_{v0}^*) \dot{\hat{K}}_{v0} + (\hat{K}_{v1} - K_{v1}^*) \dot{\hat{K}}_{v1} + (\hat{K}_{\omega2} - K_{\omega2}^*) \dot{\hat{K}}_{\omega2} \\ &= s_v (F + \epsilon_v) + (\hat{K}_{v0} - K_{v0}^*) \dot{\hat{K}}_{v0} + (\hat{K}_{v1} - K_{v1}^*) \dot{\hat{K}}_{v1} + (\hat{K}_{\omega2} - K_{\omega2}^*) \dot{\hat{K}}_{\omega2}. \end{aligned} \quad (2.21)$$

Using the control law (2.11) and the upper bound from (2.10) we have

$$\begin{aligned} \dot{V}_v &= s_v (-\Lambda_v s_v - \rho_v sgn(s_v) + \epsilon_v) + (\hat{K}_{v0} - K_{v0}^*) \dot{\hat{K}}_{v0} \\ &\quad + (\hat{K}_{v1} - K_{v1}^*) \dot{\hat{K}}_{v1} + (\hat{K}_{\omega2} - K_{\omega2}^*) \dot{\hat{K}}_{\omega2} \\ &= -\Lambda_v s_v^2 - (\hat{K}_{v0} - K_{v0}^*)(|s_v| - \dot{\hat{K}}_{v0}) - (\hat{K}_{v1} - K_{v1}^*)(|s_v| |\xi_v| - \dot{\hat{K}}_{v1}) \\ &\quad - (\hat{K}_{\omega2} - K_{\omega2}^*)(|s_w| |\xi_w| - \dot{\hat{K}}_{\omega2}). \end{aligned} \quad (2.22)$$

The adaptive laws in (2.12) yield

$$(\hat{K}_{v0} - K_{v0}^*) \dot{\hat{K}}_{v0} = |s_v| (\hat{K}_{v0} - K_{v0}^*) + \alpha_{v0} \hat{K}_{v0} K_{v0}^* - \alpha_{v0} \hat{K}_{v0}^2 \quad (2.23)$$

$$(\hat{K}_{v1} - K_{v1}^*) \dot{\hat{K}}_{v1} = |s_v| (\hat{K}_{v1} - K_{v1}^*) |\xi_v| + \alpha_{v1} \hat{K}_{v1} K_{v1}^* - \alpha_{v1} \hat{K}_{v1}^2 \quad (2.24)$$

$$(\hat{K}_{\omega2} - K_{\omega2}^*) \dot{\hat{K}}_{\omega2} = |s_w| (\hat{K}_{\omega2} - K_{\omega2}^*) |\xi_w| + \alpha_{\omega2} \hat{K}_{\omega2} K_{\omega2}^* - \alpha_{\omega2} \hat{K}_{\omega2}^2. \quad (2.25)$$

Substituting (2.23), (2.24), (2.25) into (2.22) yields

$$\begin{aligned}
\dot{V}_v &\leq -\Lambda_v |s_v|^2 + (\alpha_{v0} \hat{K}_{v0} K_{v0}^* - \alpha_{v0} \hat{K}_{v0}^2) \\
&\quad + (\alpha_{v1} \hat{K}_{v1} K_{v1}^* - \alpha_{v1} \hat{K}_{v1}^2) + (\alpha_{w2} \hat{K}_{w2} K_{w2}^* - \alpha_{w2} \hat{K}_{w2}^2) \\
&\leq -\Lambda_v |s_v|^2 - (1/2)\alpha_{v0}((\hat{K}_{v0} - K_{v0}^*)^2 - K_{v0}^{*2}) \\
&\quad - (1/2)\alpha_{v1}((\hat{K}_{v1} - K_{v1}^*)^2 - K_{v1}^{*2}) \\
&\quad - (1/2)\alpha_{w2}((\hat{K}_{w2} - K_{w2}^*)^2 - K_{w2}^{*2}).
\end{aligned} \tag{2.26}$$

Following the similar lines to obtain (2.26), one can also obtain \dot{V}_w as the following

$$\begin{aligned}
\dot{V}_w &\leq -\Lambda_w |s_w|^2 - (1/2)\alpha_{w0}((\hat{K}_{w0} - K_{w0}^*)^2 - K_{w0}^{*2}) \\
&\quad - (1/2)\alpha_{w1}((\hat{K}_{w1} - K_{w1}^*)^2 - K_{w1}^{*2}) \\
&\quad - (1/2)\alpha_{v2}((\hat{K}_{v2} - K_{v2}^*)^2 - K_{v2}^{*2}).
\end{aligned} \tag{2.27}$$

Further, using the definitions of Lyapunov function as in (2.20), (2.26) and (2.27) can be further simplified to

$$\dot{V}_v \leq -\varrho_v V_v + \frac{1}{2}(\alpha_{v0} K_{v0}^{*2} + \alpha_{v1} K_{v1}^{*2} + \alpha_{w2} K_{w2}^{*2}), \tag{2.28}$$

$$\dot{V}_w \leq -\varrho_w V_w + \frac{1}{2}(\alpha_{w0} K_{w0}^{*2} + \alpha_{w1} K_{w1}^{*2} + \alpha_{v2} K_{v2}^{*2}), \tag{2.29}$$

$$\text{where } \varrho_v \triangleq \frac{\min(\Lambda_v, \alpha_{v0}, \alpha_{v1}, \alpha_{w2})}{\max(m/2, 1/2)} > 0$$

$$\varrho_w \triangleq \frac{\min(\Lambda_w, \alpha_{w0}, \alpha_{w1}, \alpha_{v2})}{\max(J/2, 1/2)} > 0$$

Combining (2.28) and (2.29), the time derivative of the overall Lyapunov function \dot{V} can be obtained as

$$\begin{aligned}
\dot{V} &= -\varrho V + (1/2)(\alpha_{v0} K_{v0}^{*2} + \alpha_{v1} K_{v1}^{*2} + \alpha_{w2} K_{w2}^{*2}) \\
&\quad + (1/2)(\alpha_{w0} K_{w0}^{*2} + \alpha_{w1} K_{w1}^{*2} + \alpha_{v2} K_{v2}^{*2}),
\end{aligned} \tag{2.30}$$

where $\varrho \triangleq \min(\varrho_v, \varrho_w)$. Defining a scalar κ such that $0 < \kappa < \varrho$, \dot{V} in (2.30) is further simplified to

$$\begin{aligned}
\dot{V} &\leq -\kappa V - (\varrho - \kappa)V + \frac{1}{2}(\alpha_{v0} K_{v0}^{*2} + \alpha_{v1} K_{v1}^{*2} + \alpha_{w2} K_{w2}^{*2}) \\
&\quad + (1/2)(\alpha_{w0} K_{w0}^{*2} + \alpha_{w1} K_{w1}^{*2} + \alpha_{v2} K_{v2}^{*2}).
\end{aligned} \tag{2.31}$$

Defining a scalar $\beta \triangleq \frac{\sum_{i=0}^2 (\alpha_{vi} K_{vi}^*{}^2 + \alpha_{wi} K_{wi}^*{}^2)}{2(\varrho - \kappa)}$, it can be noted that $\dot{V}(t) < -\kappa V(t)$ when $V(t) \geq \beta$, leading to

$$V \leq \max(V(0), \beta), \quad \forall t > 0, \quad (2.32)$$

and hence, the closed-loop system remains UUB.

To avoid chattering due to discontinuity in control law, the ‘*sgn*’ functions in (2.11) and (2.18) are often replaced by a ‘saturation’/sigmoid functions which leads to minor modifications in the stability analysis without altering the overall UUB result and hence omitted to avoid repetition (cf. [18, 20, 29]).

Chapter 3

SIMULATION RESULTS

3.0.1 Simulation Scenario

The multi-robot platoon system operates in a decentralized manner, where each robot only requires the state information of its predecessor robot to maintain a formation (cf. Fig. 3.1). The desired waypoints for the platoon are generated using Algorithm 1, which stores the waypoints in an array. Each robot calculates its desired state based on the index number of its local leader robot in the array. Instead of calculating the shortest distance between consecutive robots, the gap between them is calculated along the path. This approach ensures that the platoon maintains a consistent formation while navigating along a given path. By using this decentralized formation control system, the multi-robot platoon can efficiently navigate through challenging environments and achieve their desired goals. The waypoints generated by Algorithm 1 provide a clear and precise path for the robots to follow, enabling them to maintain a consistent formation throughout their mission.

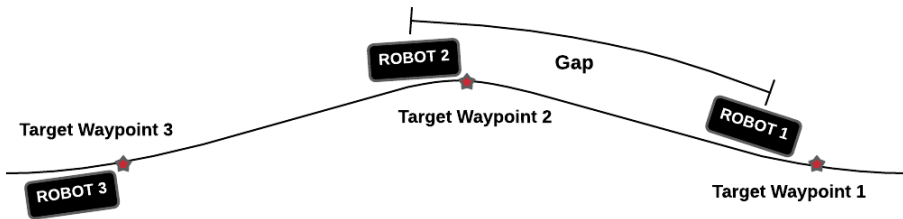


Figure 3.1: Multi-Robot Platoon Representation

Algorithm 1: Target way-point calculation

```
1 Initialisation;  
2 initialize  $d = 0$   
3 initialize  $gap_{des}$   
4  $cx$  = array containing x-coordinates of trajectory  
5  $cy$  = array containing y-coordinates of trajectory  
6  $i \leftarrow index_{leader}$   
7 while  $d < gap_{des}$  do  
8      $d+ = [(cx[i] - cx[i - 1])^2 + (cy[i] - cy[i - 1])^2]^{0.5}$   
9      $i = i - 1$   
10 end  
11 return follower  $x_r = cx[i], y_r = cy[i]$ 
```

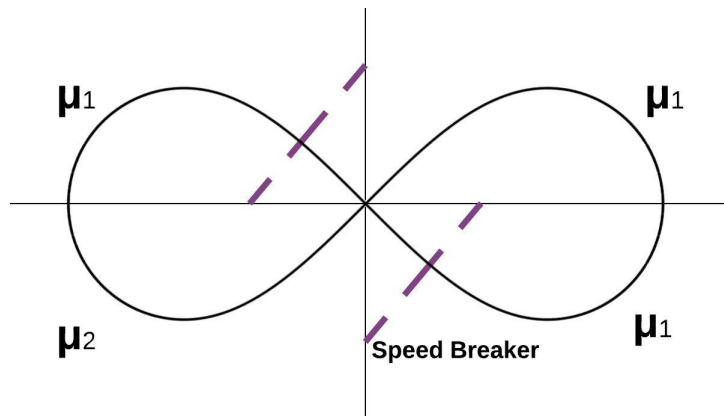


Figure 3.2: Custom Arena

The study aims to compare the performance of the proposed adaptive sliding mode controller (ASMC) with the standard ASMC [18]. The evaluation is conducted in a Gazebo simulation platform using an open-source TurtleBot3 robot model [30] and a Teeterbot plugin [31] to give a torque command to each motor using (1.11). The controller's performance is assessed in a custom arena in Gazebo ¹, which is divided into four quadrants with different surface longitudinal friction values. The first, second, and fourth quadrants have a friction value of $\mu_1 = 0.1$, while the third quadrant has a friction value of $\mu_2 = 0.13$. The lateral friction value is kept constant at 0.1 in all quadrants to prevent lateral slippage of the robots. Additionally, two speed breakers are placed in the arena to provide sudden interruptions (cf. Fig. 3.1).

Formation control is carried out using three robots, namely Robot 1, 2, and 3, which are required to follow a figure-of-eight-like path as in Fig. 3.2. The lead robot is initially positioned at coordinate (14, 0), while the follower robots are kept at a desired distance of 1m between them. The simulation platform, robot model, and plugin used in the study are all open-source and freely available.

3.0.2 Parameter Selection

For simulation, the kinematic control parameters are selected as: $k_1 = 5$, $k_2 = 3$, $k_3 = 2$, $v_d = 2$ m/sec for all robots. The control parameters of the proposed ASMC are selected to be: $\phi_v = 0.5$, $\phi_w = 0.1$, $\Lambda_v = 3$, $\Lambda_w = 2$, $\hat{K}_{v0}(0) = \hat{K}_{v1}(0) = \hat{K}_{v2}(0) = \hat{K}_{w0}(0) = \hat{K}_{w1}(0) = \hat{K}_{w2}(0) = 0.01$, $\alpha_{v0} = 2.5$, $\alpha_{v1} = 2.5$, $\alpha_{w2} = 3$, $\alpha_{w0} = 5$, $\alpha_{w1} = 5$, $\alpha_{v2} = 1.5$ for all robots. For parity, similar sliding variable and similar kinematic control parameters are designed for the standard ASMC [18].

3.0.3 Results and Analysis

The study compared the performance of two controllers, the proposed Adaptive Sliding Mode Controller (ASMC) and the standard ASMC [18] via Figs. 3.3, 3.4 and 3.5, in terms of position tracking error for three robots, labeled 1, 2, and 3. The analysis was carried out in four quadrants. In the third quadrant, between $300 < t < 400$, all robots experienced a sharp turn and high friction surface, causing an increase in tracking error. The results show that the standard ASMC [18] performed worse than the proposed ASMC during this period, as it was not designed to handle changes in state-dependent friction

¹Simulation Video: <https://youtu.be/7yHY9atSeK8>; Titled as "Adaptive Sliding Mode Control for Autonomous Vehicle Platoon under Unknown Friction Forces" on Youtube

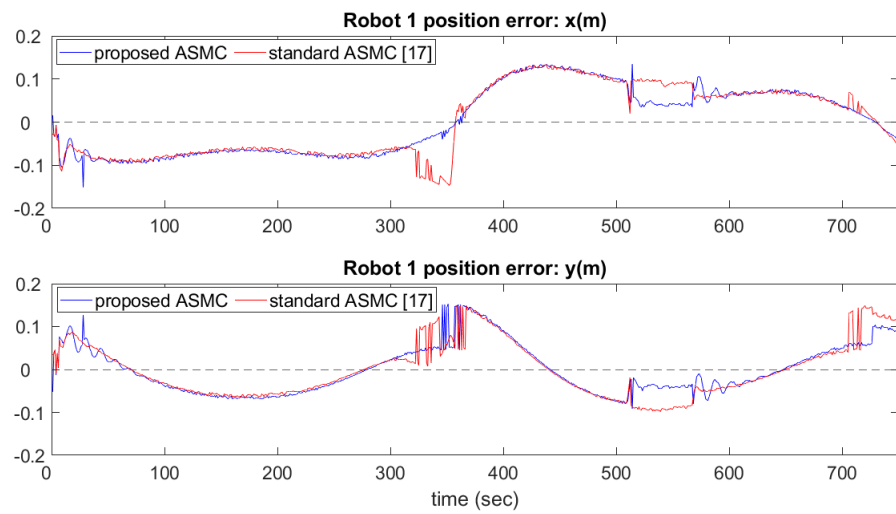


Figure 3.3: Position tracking error comparison for Robot 1.

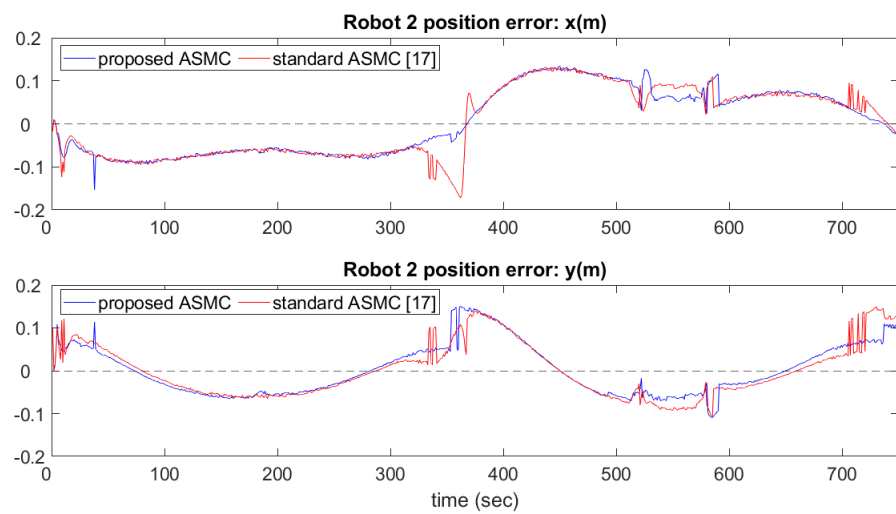


Figure 3.4: Position tracking error comparison for Robot 2.

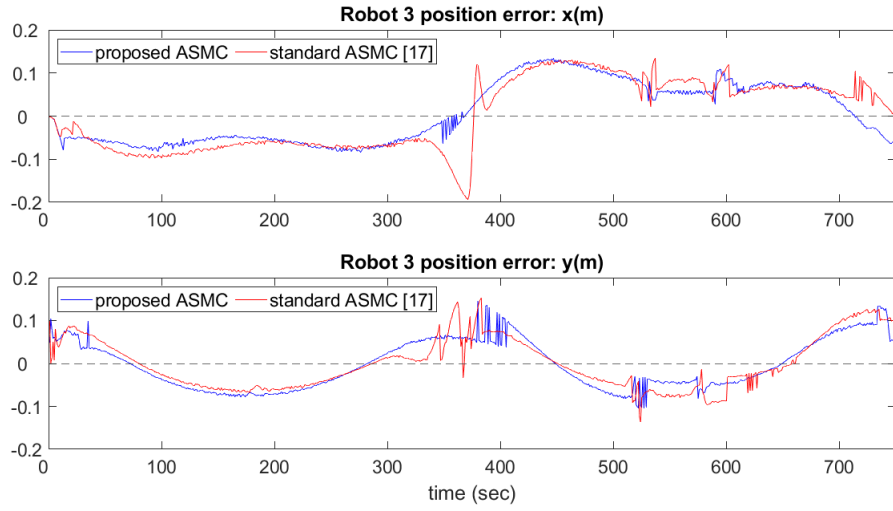


Figure 3.5: Position tracking error comparison for Robot 3.

components. A similar trend was observed between $500 < t < 600$, when the robots encountered two speed breakers. The proposed controller showed fewer spikes in the tracking error profile during this period. The performance of both controllers was found to be similar in the first, second, and fourth quadrants. This was confirmed by path tracking performances shown in Figures 3.6, 3.7 and 3.8. Overall, the results indicate that the proposed controller performs better in the third quadrant, where changes in friction components are significant, while the standard and proposed controllers have similar performance in the other quadrants.

Additionally, in Figure 3.9, the difference between the intended gap and the actual gap of two consecutive robots, namely Robot 1-Robot 2 and Robot 2-Robot 3, is illustrated, which is called the gap error. At around $t = 350$ seconds, it can be observed that when the robots are in the third quadrant and encounter a high variation in friction, the standard ASMC [18] exhibits a significantly greater gap error than the proposed ASMC. To provide more conclusive evidence, Tables 3.1 and 3.2 present the performance of both controllers in terms of root mean-squared (RMS) error. The data in these tables indicate that the proposed ASMC achieves superior tracking accuracy while preserving the desired distance between the robots.

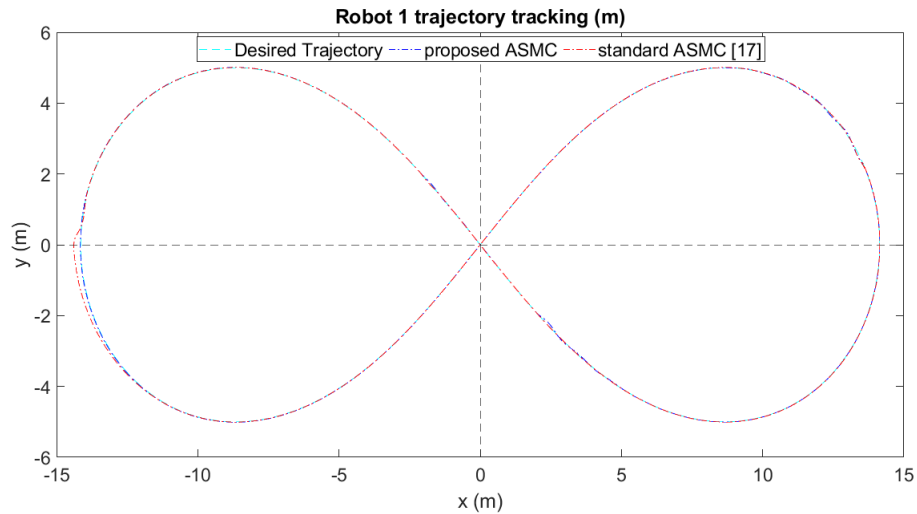


Figure 3.6: Trajectory tracking comparison for Robot 1.

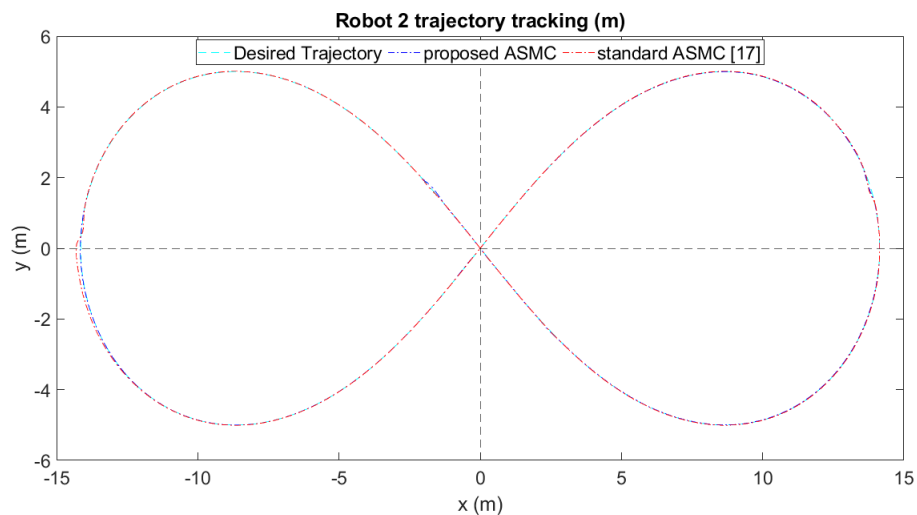


Figure 3.7: Trajectory tracking comparison for Robot 2.

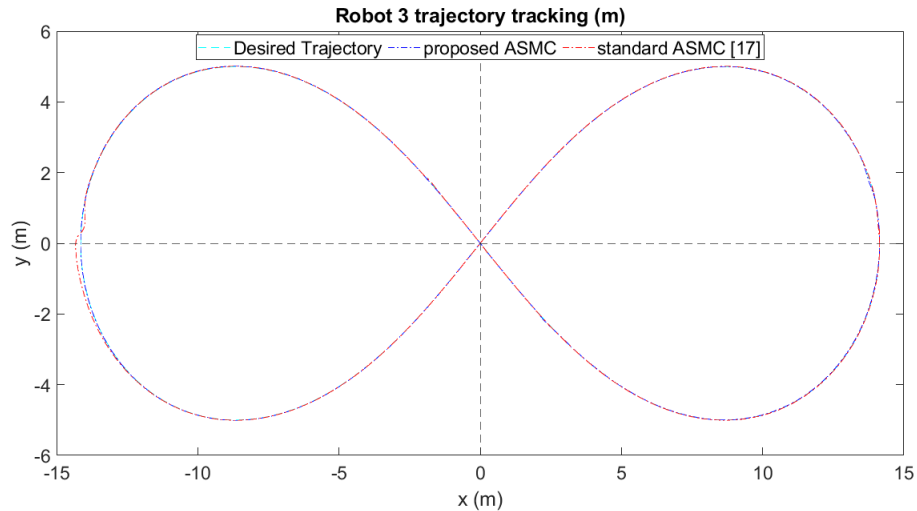


Figure 3.8: Trajectory tracking comparison for Robot 3.

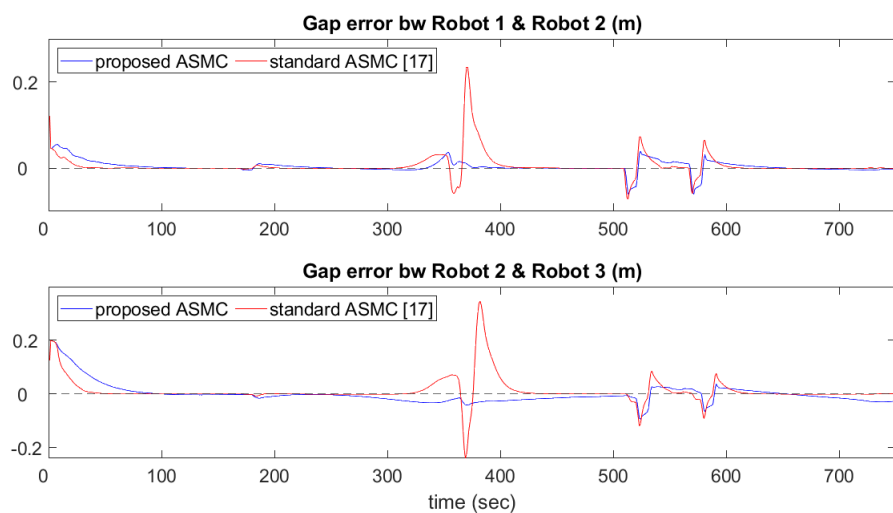


Figure 3.9: (a) Gap error comparison between Robot 1 and Robot 2. (b) Gap error comparison between Robot 2 and Robot 3.

Table 3.1: Performance Comparison for Trajectory Tracking

No.	Position	standard ASMC [17]	proposed ASMC
		RMS error (m)	RMS error(m)
Robot1	x	0.081	0.076
	y	0.063	0.056
Robot2	x	0.079	0.076
	y	0.062	0.058
Robot3	x	0.080	0.070
	y	0.060	0.056

Table 3.2: Performance Comparison for Gap Maintenance

Gap Error b/w Robots	standard ASMC [17]	proposed ASMC
	RMS error (m)	RMS error(m)
Robot 1 and Robot 2	0.026	0.014
Robot 2 and Robot 3	0.050	0.036

Chapter 4

Conclusion and Future Work

A new method has been suggested for controlling the formation of a platoon of autonomous wheeled mobile robots, which can manage factors such as external interferences, uncertainties in parameters, and variations in friction between the tire and the surface without any prior knowledge of them. The proposed adaptive sliding mode controller uses Lyapunov function to establish stability of the closed-loop system, with the help of Uniformly Ultimately Bounded concept. The effectiveness of the controller was tested under different conditions using Gazebo simulation, and the results showed significant enhancements in the performance of the platoon, in terms of both trajectory tracking and maintaining a fixed safe distance between the robots, when compared to existing methods.

The controller's ability to adjust to unknown factors, such as external disturbances, frictional differences, and parametric uncertainties, is a key feature that sets it apart from other techniques. By using a sliding mode approach, the controller's design ensures robustness and adaptation to such variations. Additionally, the Lyapunov function used in the analysis guarantees that the closed-loop system is stable, and the Uniformly Ultimately Bounded notion ensures that the solutions are bounded and convergent. The effectiveness of the proposed method was demonstrated through simulations, where it was observed that the proposed controller performed better than the existing methods, achieving high accuracy in trajectory tracking and maintaining a safe distance between the robots.

Future work involve implementing the proposed adaptive sliding mode controller on a real-world platform and conducting experiments to evaluate its performance with different slope and payloads. The controller could also be further optimized for improved energy efficiency and faster response times. Additionally, the controller's scalability could be investigated to determine its effectiveness in controlling larger platoons of mobile

robots. Finally, the proposed method could be extended to other types of autonomous systems, such as aerial drones or underwater vehicles.

Related Publications

1. Adaptive Sliding Mode Control for Autonomous Vehicle Platoon under Unknown Friction Forces [1]
R. D. Yadav*, V. Sankaranarayanan and S. Roy,
IEEE 20th International Conference on advanced robotics (ICAR 2021)

Other Publications

1. Robustifying Payload Carrying Operations for Quadrotors Under Time-Varying State Constraints and Uncertainty [32]
V. Shankaranarayanan, Rishabh Dev Yadav, R. K. Swyampakula, S. Ganguly and S. Roy
IEEE Robotics and Automation Letters, vol. 7, no. 2, pp. 4885-4892. (RAL)
2. Efficient Manoeuvring of Quadrotor under Constrained Space and Predefined Accuracy [33]
S. Ganguly, V. Sankaranarayanan, B. V. S. G. Suraj, R. D. Yadav and S. Roy
The 2021 IEEE/RSJ International Conference on Intelligent Robots and Systems (IROS 2021)
3. CCO-VOXEL: Chance Constrained Optimization over Uncertain Voxel-Grid Representation for Safe Trajectory Planning [34]
Sudarshan S Harithas, R. D. Yadav, Deepak Singh, Arun Kumar Singh, K Madhava Krishna
IEEE International Conference on Robotics and Automation (ICRA 2022)

4. Robust Manoeuvring of Quadrotor under Full State Constraints [35]
 S. Ganguly, V. Sankaranarayanan, B. V. S. G. Suraj, R. D. Yadav and S. Roy
 Automatic Control and Dynamical Optimization Society (ACDOS 2022)
5. Introducing Scissor Mechanism based Novel Reconfigurable Quadrotor: Design, Modelling and Control [36]
 B. V. S. G. Suraj, Viswa N. Sankaranarayanan, Rishabh Dev Yadav and Spandan Roy,
 IEEE International Conference on Robotics and Biomimetics (ROBIO 2022)
6. Adaptive Artificial Time Delay Control for Quadrotors under State-dependent Unknown Dynamic [37]
 Swati Dantu, R. D. Yadav, Spandan Roy, Jinoh Lee and Simone Baldi
 IEEE International Conference on Robotics and Biomimetics (ROBIO 2022)
7. Adaptive Anti-swing Control for Clasping Operations in Quadrotors with Cable-suspended Payload [38]
 S. Dantu, R. D. Yadav, A. Rachakonda, S. Roy, S. Baldi
 IEEE Conference on Decision and Control (CDC 2023)
8. An Integrated Approach to Aerial Grasping: Combining a Bistable Gripper with Adaptive Control [39]
 Rishabh Dev Yadav, Brycen Jones, Saksham Gupta, Amitabh Sharma, Jiefeng Sun, Jianguo Zhao, Spandan Roy
 IEEE/ASME Transactions on Mechatronics

Bibliography

- [1] Rishabh Dev Yadav, Viswa N Sankaranarayanan, and Spandan Roy. Adaptive sliding mode control for autonomous vehicle platoon under unknown friction forces. In 2021 20th International Conference on Advanced Robotics (ICAR), pages 879–884. IEEE, 2021.
- [2] Rachael N Darmanin and Marvin K Bugeja. A review on multi-robot systems categorised by application domain. In 25th Mediterranean Conference on Control and Automation, pages 701–706. IEEE, 2017.
- [3] Tamio Arai, Enrico Pagello, Lynne E Parker, et al. Advances in multi-robot systems. *IEEE Transactions on Robotics and Automation*, 18(5):655–661, 2002.
- [4] Zool Hilmi Ismail and Nohaidda Sariff. A survey and analysis of cooperative multi-agent robot systems: Challenges and directions. In *Applications of Mobile Robots*, pages 8–14. IntechOpen, 2018.
- [5] Yifan Cai and Simon X Yang. A survey on multi-robot systems. In *World Automation Congress 2012*, pages 1–6. IEEE, 2012.
- [6] Jorge Cortés and Magnus Egerstedt. Coordinated control of multi-robot systems: A survey. *SICE Journal of Control, Measurement, and System Integration*, 10(6):495–503, 2017.
- [7] Aakash Soni and Huosheng Hu. Formation control for a fleet of autonomous ground vehicles: A survey. *Robotics*, 7(4):67, 2018.
- [8] Gianluca Antonelli and Stefano Chiaverini. Kinematic control of platoons of autonomous vehicles. *IEEE Transactions on Robotics*, 22(6):1285–1292, 2006.
- [9] Shi-Lu Dai, Shude He, Hai Lin, and Cong Wang. Platoon formation control with prescribed performance guarantees for usvs. *IEEE Transactions on Industrial Electronics*, 65(5):4237–4246, 2017.

- [10] Karl Berntorp, Rien Quirynen, and Stefano Di Cairano. Steering of autonomous vehicles based on friction-adaptive nonlinear model-predictive control. In American Control Conference, pages 965–970. IEEE, 2019.
- [11] Claudiu Iurian, Fayçal Ikhouane, José Rodellar Benedé, and Robert Griñó Cubero. Identification of a system with dry friction. 2005.
- [12] J Čerkala and A Jadlovska. Mobile robot dynamics with friction in simulink. In Proceedings of the 22th Annual Conference Proceedings of the International Scientific Conference—Technical Computing Bratislava, pages 1–10, 2014.
- [13] Alon Tuchner and Jack Haddad. Vehicle platoon formation using interpolating control: A laboratory experimental analysis. *Transportation Research Part C: Emerging Technologies*, 84:21–47, 2017.
- [14] Liwei Xu, Weichao Zhuang, Guodong Yin, and Chentong Bian. Distributed formation control of homogeneous vehicle platoon considering vehicle dynamics. *International Journal of Automotive Technology*, 20(6):1103–1112, 2019.
- [15] Jilie Zhang, Tao Feng, Fei Yan, Shaojie Qiao, and Xiaomin Wang. Analysis and design on intervehicle distance control of autonomous vehicle platoons. *ISA Transactions*, 100:446–453, 2020.
- [16] Xiaomin Zhao, YH Chen, and Han Zhao. Robust approximate constraint-following control for autonomous vehicle platoon systems. *Asian Journal of Control*, 20(4):1611–1623, 2018.
- [17] Chih-Yang Chen, Tzuu-Hseng S Li, Ying-Chieh Yeh, and Cha-Cheng Chang. Design and implementation of an adaptive sliding-mode dynamic controller for wheeled mobile robots. *Mechatronics*, 19(2):156–166, 2009.
- [18] Muhammad Asif, Muhammad Junaid Khan, and Ning Cai. Adaptive sliding mode dynamic controller with integrator in the loop for nonholonomic wheeled mobile robot trajectory tracking. *International Journal of Control*, 87(5):964–975, 2014.
- [19] Yasmine Koubaa, Mohamed Boukattaya, and Tarak Damak. Adaptive sliding mode control for trajectory tracking of nonholonomic mobile robot with uncertain kinematics and dynamics. *Applied Artificial Intelligence*, 32(9-10):924–938, 2018.

- [20] Spandan Roy, Sayan Basu Roy, Jinoh Lee, and Simone Baldi. Overcoming the underestimation and overestimation problems in adaptive sliding mode control. *IEEE/ASME Transactions on Mechatronics*, 24(5):2031–2039, 2019.
- [21] Vadim I Utkin and Alex S Poznyak. Adaptive sliding mode control with application to super-twist algorithm: Equivalent control method. *Automatica*, 49(1):39–47, 2013.
- [22] Rafael Fierro and Frank L Lewis. Control of a nonholomic mobile robot: Backstepping kinematics into dynamics. *Journal of robotic systems*, 14(3):149–163, 1997.
- [23] José Rafael García-Sánchez et al. Tracking control for mobile robots considering the dynamics of all their subsystems: Experimental implementation. *Complexity*, 2017, 2017.
- [24] Kang Liu, Hongbo Gao, Haibo Ji, and Zhengyuan Hao. Adaptive sliding mode based disturbance attenuation tracking control for wheeled mobile robots. *International Journal of Control, Automation and Systems*, 18(5):1288–1298, 2020.
- [25] Spandan Roy and Simone Baldi. Towards structure-independent stabilization for uncertain underactuated euler–lagrange systems. *Automatica*, 113:108775, 2020.
- [26] Spandan Roy, Simone Baldi, and Leonid M Fridman. On adaptive sliding mode control without a priori bounded uncertainty. *Automatica*, 111:108650, 2020.
- [27] Spandan Roy, Simone Baldi, and Petros A Ioannou. An adaptive control framework for underactuated switched euler-lagrange systems. *IEEE Transactions on Automatic Control*, 2021.
- [28] Harsh Shukla, Spandan Roy, and Satyam Gupta. Robust adaptive control of steer-by-wire systems under unknown state-dependent uncertainties. *International Journal of Adaptive Control and Signal Processing*, 2021.
- [29] Spandan Roy, Jinoh Lee, and Simone Baldi. A new adaptive-robust design for time delay control under state-dependent stability condition. *IEEE Transactions on Control Systems Technology*, 29(1):420–427, 2020.
- [30] ROBOTIS-GIT. Turtlebot3.
- [31] Robustify. Teeterbot: Self-balancing robot.

- [32] Viswa N Sankaranarayanan, Rishabh D Yadav, Rahul K Swayampakula, Sourish Ganguly, and Spandan Roy. Robustifying payload carrying operations for quadrotors under time-varying state constraints and uncertainty. *IEEE Robotics and Automation Letters*, 7(2):4885–4892, 2022.
- [33] Sourish Ganguly, Viswa N Sankaranarayanan, BVSG Suraj, Rishabh Dev Yadav, and Spandan Roy. Efficient manoeuvring of quadrotor under constrained space and predefined accuracy. In 2021 IEEE/RSJ International Conference on Intelligent Robots and Systems (IROS), pages 6352–6357. IEEE, 2021.
- [34] Sudarshan S Harithas, Rishabh Dev Yadav, Deepak Singh, Arun Kumar Singh, and K Madhava Krishna. Cco-voxel: Chance constrained optimization over uncertain voxel-grid representation for safe trajectory planning. In 2022 International Conference on Robotics and Automation (ICRA), pages 11087–11093. IEEE, 2022.
- [35] Sourish Ganguly, Viswa N Sankaranarayanan, BVSG Suraj, Rishabh Dev Yadav, and Spandan Roy. Robust manoeuvring of quadrotor under full state constraints. *IFAC-PapersOnLine*, 55(1):32–37, 2022.
- [36] BVSG Suraj, Viswa N Sankaranarayanan, Rishabh Dev Yadav, and Spandan Roy. Introducing scissor mechanism based novel reconfigurable quadrotor: Design, modelling and control. In 2022 IEEE International Conference on Robotics and Biomimetics (ROBIO), pages 2231–2236. IEEE, 2022.
- [37] Swati Dantu, Rishabh Dev Yadav, Spandan Roy, Jinoh Lee, and Simone Baldi. Adaptive artificial time delay control for quadrotors under state-dependent unknown dynamics. In 2022 IEEE International Conference on Robotics and Biomimetics (ROBIO), pages 1092–1097. IEEE, 2022.
- [38] Swati Dantu, Rishabh Dev Yadav, Ananth Rachakonda, Spandan Roy, and Simone Baldi. Adaptive anti-swing control for clasping operations in quadrotors with cable-suspended payload. In 2023 62nd IEEE Conference on Decision and Control (CDC), pages 503–508. IEEE, 2023.
- [39] Rishabh Dev Yadav, Brycen Jones, Saksham Gupta, Amitabh Sharma, Jiefeng Sun, Jianguo Zhao, and Spandan Roy. An integrated approach to aerial grasping: Combining a bistable gripper with adaptive control, 2023.